Genes & Diseases (2022) 9, 230–244

Available online at www.sciencedirect.com

ScienceDirect

journal homepage: http://ees.elsevier.com/gendis/default.asp

FULL LENGTH ARTICLE

PRR11 induces filopodia formation and promotes cell motility via recruiting ARP2/3 complex in non-small cell lung cancer cells

Zhili Wei [a,b], Ru Wang [a,b], Xun Yin [a,b], lian Zhang [a,b,c], Yunlong Lei [a,b], Ying Zhang [a,b], Yi Li [a,b], Jiaqian Wu [a,b], Youquan Bu [a,b], Guoxiang Jin [c], Chundong Zhang [a,b,*]

[a] *Department of Biochemistry and Molecular Biology, Chongqing Medical University, Chongqing 400016, PR China*
[b] *Molecular Medicine and Cancer Research Center, Chongqing Medical University, Chongqing 400016, PR China*
[c] *Guangdong Provincial People's Hospital, Guangdong Academy of Medical Sciences, Guangzhou, Guangdong 510080, PR China*

Received 27 September 2020; received in revised form 25 January 2021; accepted 21 February 2021
Available online 2 March 2021

KEYWORDS
ARP2/3 complex;
Cell motility;
FAK;
Filopodia;
Focal adhesion;
Integrin;
NSCLC cells;
PRR11

Abstract Filopodia, a finger-like structure and actin-rich plasma-membrane protrusion at the leading edge of the cell, has important roles in cell motility. However, the mechanisms of filopodia generation are not well-understood via the actin-related protein 2/3 (ARP2/3) complex in Non-Small Cell Lung Cancer (NSCLC) cells. We previously have demonstrated that PRR11 associates with the ARP2/3 complex to regulate cytoskeleton-nucleoskeleton assembly and chromatin remodeling. In this study, we further demonstrate that PRR11 involves in filopodia formation, focal adhesion turnover and cell motility through ARP2/3 complex. Cell phenotype assays revealed that the silencing of PRR11 increased cellular size and inhibited cell motility in NSCLC cells. Mechanistically, PRR11 recruited and co-localized with Arp2 at the membrane protrusion to promote filopodia formation but not lamellipodia formation. Notably, PRR11 mutant deletion of the proline-rich region 2 (amino acid residues 185–200) abrogated the effect of filopodia formation. In addition, PRR11-depletion inhibited filopodial actin filaments assembly and increased the level of active integrin β1 in the cell surface, whereas reduced the phosphorylation level of focal adhesion kinase (FAK^{Y397}) to repress focal adhesion turnover and cell motility in NSCLC cells. Taken together, our findings indicate that PRR11 has critical roles in controlling filopodia formation, focal adhesion turnover and cell motility by recruiting ARP2/

* Corresponding author. Department of Biochemistry and Molecular Biology, Chongqing Medical University, 1# Yixueyuan Road, Yuzhong District, Chongqing 400016, PR China.
E-mail address: zhangcd@cqmu.edu.cn (C. Zhang).
Peer review under responsibility of Chongqing Medical University.

https://doi.org/10.1016/j.gendis.2021.02.012

3 complex, thus dysregualted expression of PRR11 potentially facilitates tumor metastasis in NSCLC cells.

Introduction

Lung cancer is the most common cause of cancer-related deaths worldwide, and Non-Small-Cell Lung Cancer (NSCLC) accounts for 85%—90% of all lung cancer cases.[1] Despite some advances in early detection and recent improvements in treatment, the 5-year survival rates for lung cancer remain low (16%) for all stages.[1,2] Metastasis is the most devastating stage of tumorigenesis and causes high mortalities.[2] Metastasis contains multiple sequential and interrelated steps, and is regulated by various signaling pathways. There is considerable interest in understanding the molecular basis of cell motility because this could lead to new therapeutic strategies for cancer metastasis.[2] Aberrant actin filaments assembly induces membrane protrusion and promotes focal adhesion turnover to induce cell motility in cancer metastasis.[3] However, not much is known about specific molecular mechanisms underpinning actin filaments and cell motility in cancer progression.

Cell motility is critical to many physiological and pathological processes, including embryogenesis, the inflammatory response and cancer metastasis.[3] Cell motility can be viewed as a multistep cycle, including membrane protrusion of the cell front, the leading edge of the protrusion attachment extracellular matrix (ECM), movement of the nuclear forward, disassembly of adhesions and retraction at the cell rear.[4] During cell motility, actin filaments assembly of filopodia and lamellipodia induces membrane protrusion, which is promoted by the actin nucleator, such as actin-related protein 2/3 (ARP2/3) complex, ENA/Vasp and formins.[5] Following the actin filaments assembly of filopodia and lamellipodia, integrin-containing membrane protrusion forms adhesion site.[6] Focal adhesions connect actin cytoskeleton of membrane protrusion to ECM, which are heterodimeric receptors of the integrin-based, a dynamic plasma membrane-associated multi-molecular complexes, and are actually tightly coupled both spatially and temporally.[5] Reports have demonstrated that actin filaments of filopodia and lamellipodia regulate components of focal adhesion complex to control focal adhesion turnover and cell motility, such as conformation changes and internalization of integrin and phosphorylation of focal adhesion kinase (FAK).[6,7] And inhibition of the actin filaments assembly in the membrane protrusions impairs cell motility in various cells.[4,7–9] To date, the underlying molecular mechanisms that underlie cell motility are still incompletely understood.

We have previously demonstrated that PRR11 is implicated in lung cancer development.[10–12] PRR11-depletion causes the dysregulation of multiple critical pathways and various important genes involved in cell cycle, tumorigenesis and metastasis in NSCLC cells. Moreover, PRR11 also play critical roles in gastric cancer, breast cancer and hilar cholangiocarcinoma.[13–15] Recently, we have demonstrated that cytoplasmic PRR11 associates with and recruits ARP2/3 complex to effect on cytoskeleton-nucleoskeleton assembly and chromatin remodeling.[16] In this study, we further demonstrate that PRR11 regulates the actin filaments assembly of filopodia by recruiting ARP2/3 complex, and promoted focal adhesions turnover and cell motility. Our study reveals that PRR11 serves as a novel factor regulating filopodia formation, focal adhesions dynamic and cell motility in NSCLC cells.

Materials and methods

Cell culture

Human non-small cell lung carcinoma-derived H1299 and A549 were obtained from the ATCC. Cells were cultured in RPMI 1640 medium and Dulbecco's modified Eagle's medium (DMEM), respectively, supplemented with 10% heat-inactivated fetal bovine serum (GIBCO) and penicillin (100 IU/ml)/streptomycin (100 mg/ml). Cells were maintained at 37 °C in a water-saturated atmosphere of 5% CO_2 in air. For the detection of mycoplasma in the cell cultures, we used MYCOPLASMA STAIN KIT (Mpbio, California, USA). CK-666 was purchased from SIGMA-ALDRICH.

Transient transfection

For transient transfection, cells were seeded at a density of 0.8×10^5 cells/well in a 24-well tissue culture plate or 2.5×10^5 cells/well in a 6-well tissue culture plate and incubated overnight. Cells were then transiently transfected with the indicated plasmids using Lipofectamine 2000 transfection reagent (Invitrogen) following the manufacturer's protocols.

siRNA-mediated knockdown

The nucleotide sequences of control siRNA and specific against PRR11 and ARPC1 siRNA were described previously or were designed by Online tools (Invitrogen)[16] (Table S1). Prior to transfection, cells were seeded at a density of 5×10^4 cells/well in a 24-well tissue culture plate or 2×10^5 cells/well in a 6-well tissue culture plate and allowed to attach overnight. The indicated siRNAs were then transiently transfected into cells using Lipofectamine RNAiMAX transfection reagent (Invitrogen) according to the manufacturer's instructions.

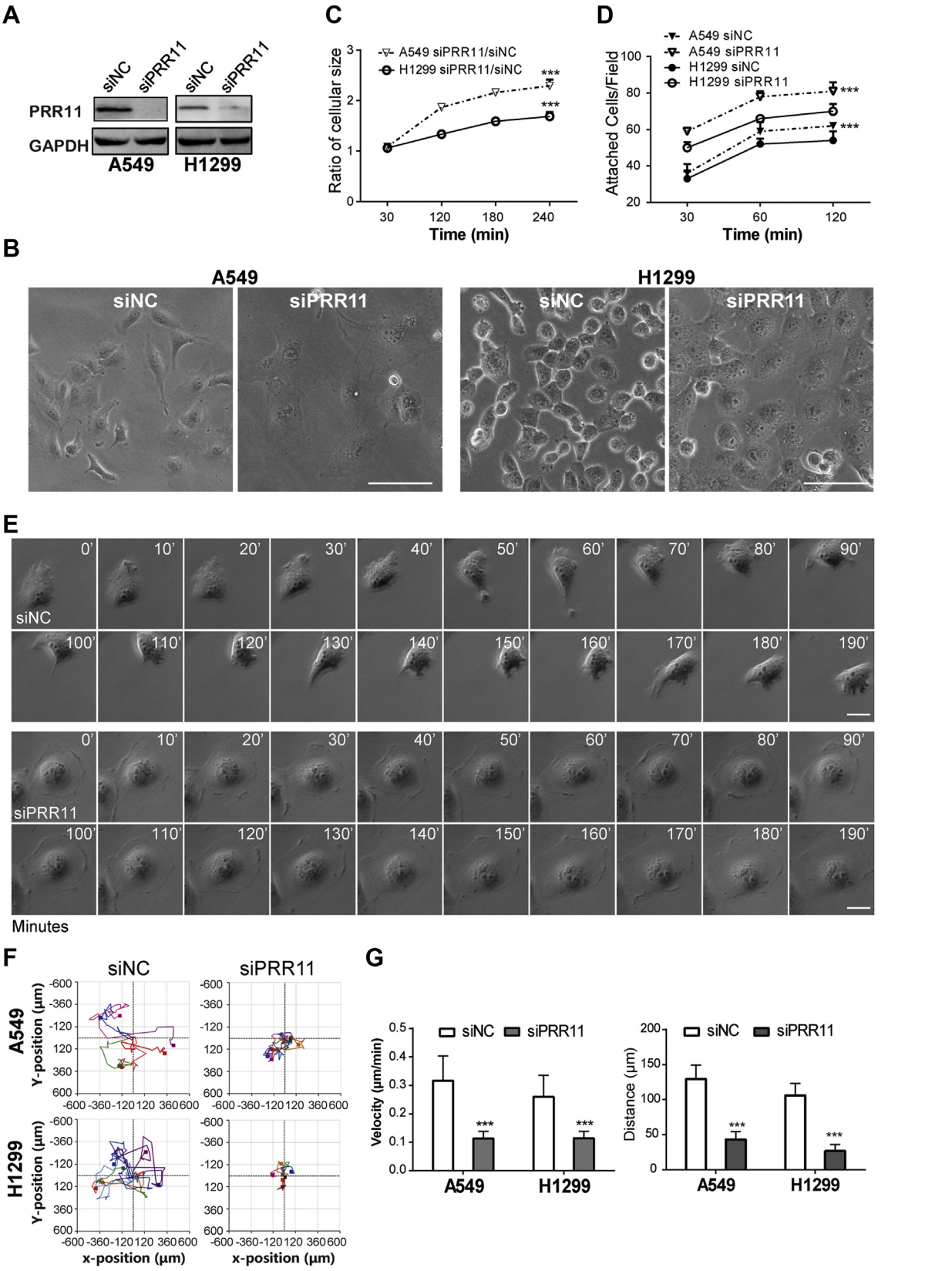

Figure 1 Silencing of PRR11 inhibits cell motility in NSCLC cells. (**A**) siRNA-mediated silencing of PRR11. A549 or H1299 cells were transiently transfected with a negative control siRNA (siNC) or with siRNA against PRR11. Forty-eight hours after transfection, whole-cell lysates were prepared and analyzed the expression of the indicated proteins. GAPDH, glyceraldehyde-3-phosphate dehydrogenase. (**B**) The effects of PRR11 depletion with the cell morphology. A549 and H1299 cells were transiently transfected

Construction of expression plasmids and transient transfection

The entire or the truncated coding sequence of human PRR11 was inserted into the mammalian expression plasmid pcDNA3.0 along with an N-terminal Flag-tag. After sequencing to confirm the accuracy of the resulting sequences, these constructs were designated as WT PRR11 (pcDNA-PRR11), Δ33-41 (deletion of residues 33—41), Δ185-200 (deletion of residues 185—200) (The primers used for construction of expression plasmids are listed in Table S1). pvN173 (Flag-tagged N-terminal 173 residues of enhanced GFP) was obtained from Dr. Cheng Lu, State Key Laboratory of Silkworm Genome Biology, Southwest University, China.

For transient transfection, cells were seeded at a density of 0.8×10^5 cells/well in a 24-well tissue culture plate or 2.5×10^5 cells/well in a 6-well tissue culture plate and incubated overnight. Cells were then transiently transfected with the indicated plasmids using Lipofectamine 2000 transfection reagent (Invitrogen) following the manufacturer's protocols.

Stable overexpression/knockdown cell line generation

For stable mCherry-Zyxin-expressing A549 cells, the entire coding sequence of Zyxin was inserted into the lentivirus-mediated plasmid pCDH-pure-mCherry. The lentivirus particles were packaged and prepared by cotransfection of the lentiviral vectors, psPax2 and pMD2.G vectors (Shanghai Genechem) into 293T cells by Lipofectamine 2000 (Invitrogen), followed by routine culture supernatant collection and concentration. The lentivirus particles carrying pCDH -mCherry-Zyxin were used to infect A549 cells. Forty-eight hours after infection, cells were selected in the presence of puromycin for about two weeks to generate the pCDH-mCherry-Zyxin stable overexpression cells, designated as mCherry-Zyxin, respectively.

For RNAi lentivirus production and infection, based on the corresponding siRNA sequences (Table S1) used in the transient transfection experiment, the stem-loop DNA oligonucleotides for PRR11 as well as the negative control shRNAs were designed, synthesized, and cloned into the lentivirus-based RNAi vector pLKO-puro (Puromycin, Addgene). The lentiviral RNAi vector and the packaging plasmids (VSVG, PLP1 and PLP2, Invotrgen) were co-transfected into the packaging cell line 293T. Viral supernatants were collected 48 h later, centrifuged to remove cell debris, filtered through 0.45-μm filters (Millipore), and concentrated using Amicon Ultra centrifugal filters (100 kDa MWCO, Millipore). The concentrated virus with the siRNA of interest was used to infect target cells. The infected cells were then sub-cultured and selected according to the presence of puromycin for generating the negative control, PRR11 and ARPC1A.

Indirect immunofluorescence staining

Cells were fixed and incubated with primary antibodies, followed by incubation with Alexa 488/594-conjugated secondary antibodies (Table S2). Cells were then mounted with medium containing 4′6-diamidino-2-phenylindole (DAPI; Sigma), and the preparations were visualized with a Leica fluorescence microscope and a Zeiss confocal LSM 768 microscope. Pixels quantification was performed using the Image J software. The antibodies used for immunofluorescence assays are listed in Table S2.

Immunoblotting analysis

Cells were lysed in RIPA lysis buffer (50 mM Tris—HCl, pH 7.4; 150 mM NaCl; 0.1% SDS; 1% NP-40 and 0.5% deoxycholate; Santa Cruz Biotechnology) supplemented with protease inhibitor mixture (Roche Applied Science). For nuclear and cytoplasmic separation, the cells were incubated with lysis buffer on ice for 5 min. The samples were spun down at 4 °C for 15 min at full speed, and the supernatants were collected as cytoplasmic fractions. The pellets were washed with lysis buffer twice and sonicated in the lysis buffer to obtain the nuclear fractions. The protein concentration of each lysate was determined by BCA reagent (Applygen Technologies). Equal amounts of the lysates (30 μg of protein) were denatured at 100 °C for 5 min, separated by 10% standard SDS-PAGE and electrotransferred onto polyvinylidene difluoride membranes (Millipore). The membranes were blocked with 5% non-fat dry milk in Tris-buffered saline (TBS) containing 0.1% Tween 20 at 4 °C overnight. After blocking, the membranes were then probed with the indicated primary antibodies at room temperature for 1 h, followed by incubation with the corresponding horseradish peroxidase-conjugated secondary antibodies at room temperature for 1 h. The proteins were finally visualized by enhanced chemiluminescence (Amersham). The antibodies used in this study are listed in Table S2.

as in (**A**). Forty-eight hours after transfection, cells were photographed. Scale bar, 50 μm. (**C**) Quantified cellular area in siRNA treatment cells. A549 cells were transiently transfected as in (**A**). Forty-eight hours after transfection, cells were placed into the 6 cm dish. Cellular area were quantified with ImageJ and shown as line graphs. $n = 3$. Greater than 50 cells were counted per condition in every repeat. ***, $P < 0.001$. (**D**) Quantified of attached cells/field in PRR11 depletion cells. A549 and H1299 cells were transiently transfected as in (**A**). Forty-eight hours after transfection cells were placed into the 6 cm dish. Attached cells/field were quantified with ImageJ and shown as line graphs. $n = 3$. Greater than 50 cells were counted per condition in every repeat. ***, $P < 0.001$. (**E**—**G**) Movements of individual A549 cells were traced by videomicroscopy. A549 cells were transiently transfected as in (**A**). Forty-eight hours after transfection, cells were placed into the confocal dish to photograph by Time-lapse confocal microscopy. Representative images are shown in (**E**). Cell migration trajectories were then recorded. $n = 5$ (**F**). The velocity of cell migration and the distance from (**E**) were analyzed with the ImageJ software and shown as the mean ± S.E. ($n = 3$) (**G**). Scale bar, 50 μm ***, $P < 0.001$.

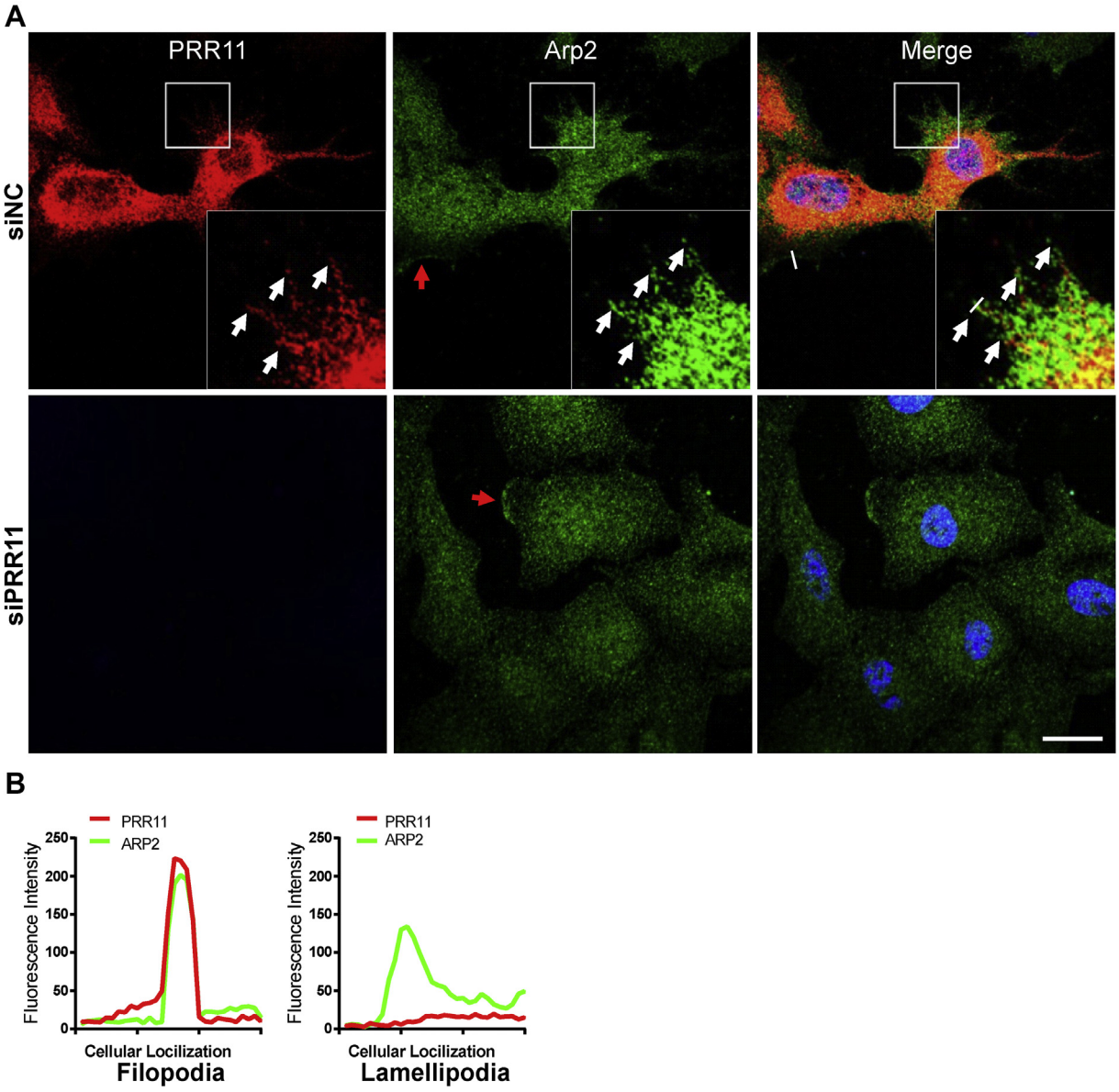

Figure 2 PRR11 recruits Arp2/3 complex moving toward the filopodia. (**A**) The subcellular localization of endogenous PRR11 and Arp2. A549 cells transiently transfected with siNC and siPRR11 were fixed after 48 h, and stained with PRR11 and Arp2 antibody. Cell nuclei were stained with DAPI (blue). Scale bars, 20 μm. And zoomed images of the boxed region are shown at the bottom-right corner. White arrowhead indicates that PRR11 and Arp2 co-localizes at the filopodia. Red arrowhead indicates that Arp2 localizes at the lamellipodia. (**B**) Co-localization analysis of PRR11 and Arp2 fluorescence signal from (**A**) was performed. The line graphs represent overlap between PRR11 and Arp2 signal at the filopodia (left panel) or PRR11 and Arp2 signal at the lamellipodia (right panel) (the white line from (**A**)).

Tissue microarray and immunohistochemistry

PRR11 and FAK^{Y397} protein expression was determined on a lung cancer tissue microarray slide from SHANGHAI OUTDO BIOTECH CO.,LTD (Shanghai; OD-CT-RsLug04-005). RsLug04 contains five adjacent normal tissue and 40 NSCLC tissues. For immunohistochemistry, slides were routinely deparaffinized and rehydrated, and then were subjected to heat-induced epitope retrieval in 0.01 mM citrate buffer (pH 6.0). Endogenous peroxidase activity was blocked for 10 min in 3% hydrogen peroxide and methanol. The slides were then incubated with PRR11 rabbit polyclonal antibody (1:150; Sigma—Aldrich Co.; HPA023923) or FAK^{Y397} Rabbit monoclonal (1:100; Abcam.; EP2160Y)at 4 °C overnight.

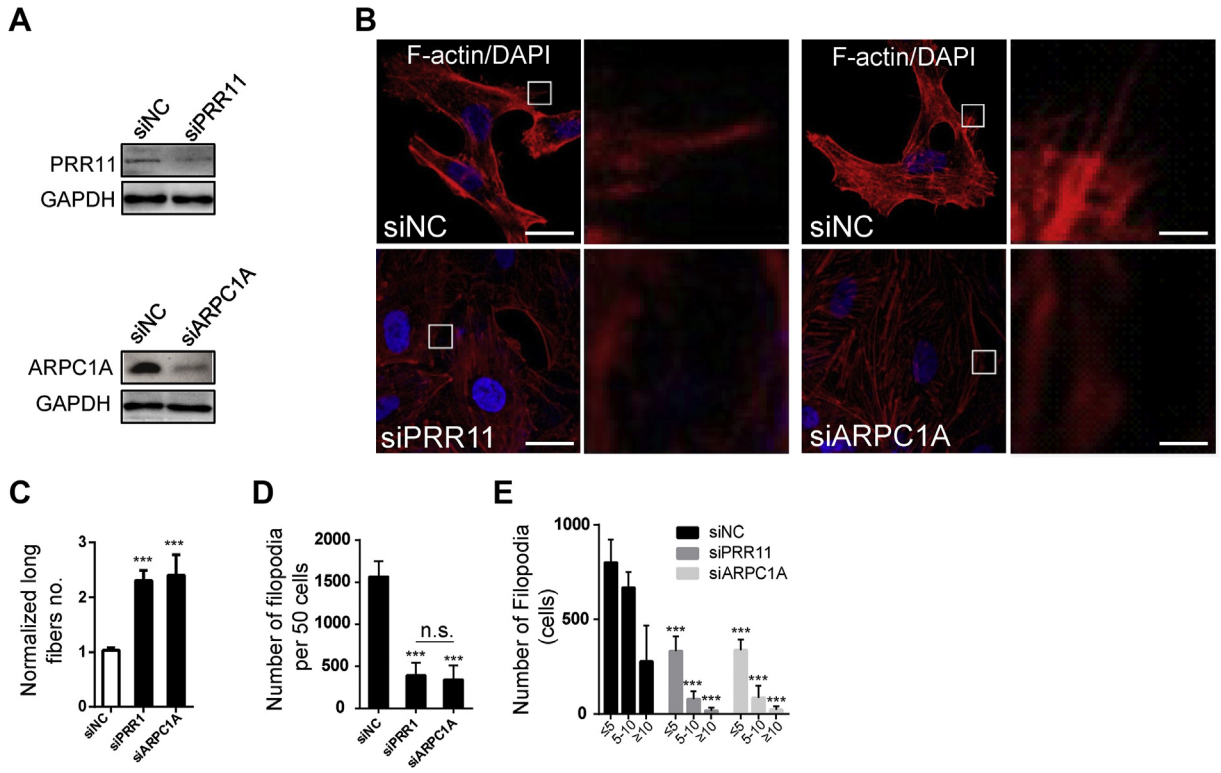

Figure 3 PRR11 induces the filopodia formation depending on Arp2/3 complex. (**A**) siRNA-mediated silencing of PRR11 and ARPC1A. A549 cells transfected with siNC or siRNA directed against PRR11 and ARPC1A. Whole-cell lysates were prepared to analyze the expression of the indicated proteins 48 h after transfection. (**B**) PRR11 and ARPC1A knockdown suppressed actin filaments assembly of filopodia. A549 cells were transiently transfected as in (**A**). Forty-eight hours after transfection, the siNC-, siPRR11-and siARPC1A-transfected cells were fixed and stained with F-actin-binding phalloidin-TRITC (red). Representative images are shown. Cell nuclei were stained with DAPI (blue). Bars, 20 μm. (**C**) Quantification of the number of rearranged long filament actin following the siRNA treatment described as in (**B**). ***, $P < 0.001$. (**D, E**) Quantified of the number and length of filopodia. The number and length of filopodia were quantified by automated scanning in the siNC-, siPRR11-and siARPC1A-transfected cells using confocal microscopy. We counted all filopodia from per cell, and the length of each tentacle was measured from the cell surface to the tip of the filopodia. Results are shown as the mean ± S.E. ($n = 3$). Greater than 50 cells were counted per condition in every repeat. *n.s*, $P > 0.05$; ***, $P < 0.001$.

Immunodetection was performed using ElivisionTM plus Polyer HRP (Mouse/Rabbit) IHC Kit (Maixin. Bio, Fuzhou, China; KIT-9902). Diaminobenzidine (Maixin. Bio, Fuzhou, China; DAB-0031/1031) was used for color development, and hematoxylin was used for counterstaining. Negative control was performed using normal rabbit IgG.

Attachment assay

Forty-eight hours after siRNA transiently transfected, A549 and H1299 cells were grown added to dish for indicated times. The number of cells/field attached to dish, and cellular size was detected from 3 to 4 fields/well, respectively.

Statistical analysis

Statistical analyses were performed using Graph-Pad Prism (http://www.graphpad.com/). Data were expressed as the means ± SEM of the values from the independent experiments performed, as indicated in the corresponding figure legends. The numbers of biological replicates, and what they represent, are indicated in each figure legend. Two-tailed Student's *t* tests were used for single comparison and two-way ANOVA was used for multiple comparisons. In all figures, statistical significance between the indicated sample and control or between marked pairs are designated: $^{*}P < 0.05$, $^{**}P < 0.01$, $^{***}P < 0.001$, or N.S. ($P > 0.05$, refers to no significant difference).

Results

Depletion of PRR11 expression increases cell adhesion and represses cell motility in NSCLC cells

Our recent studies have demonstrated that PRR11 associates with and recruits ARP2/3 complex to promote the actin filaments assembly.[16] The Arp2/3 complex drives branched actin filament networks, which plays critical roles in several processes, including the formation of protrusions for cell

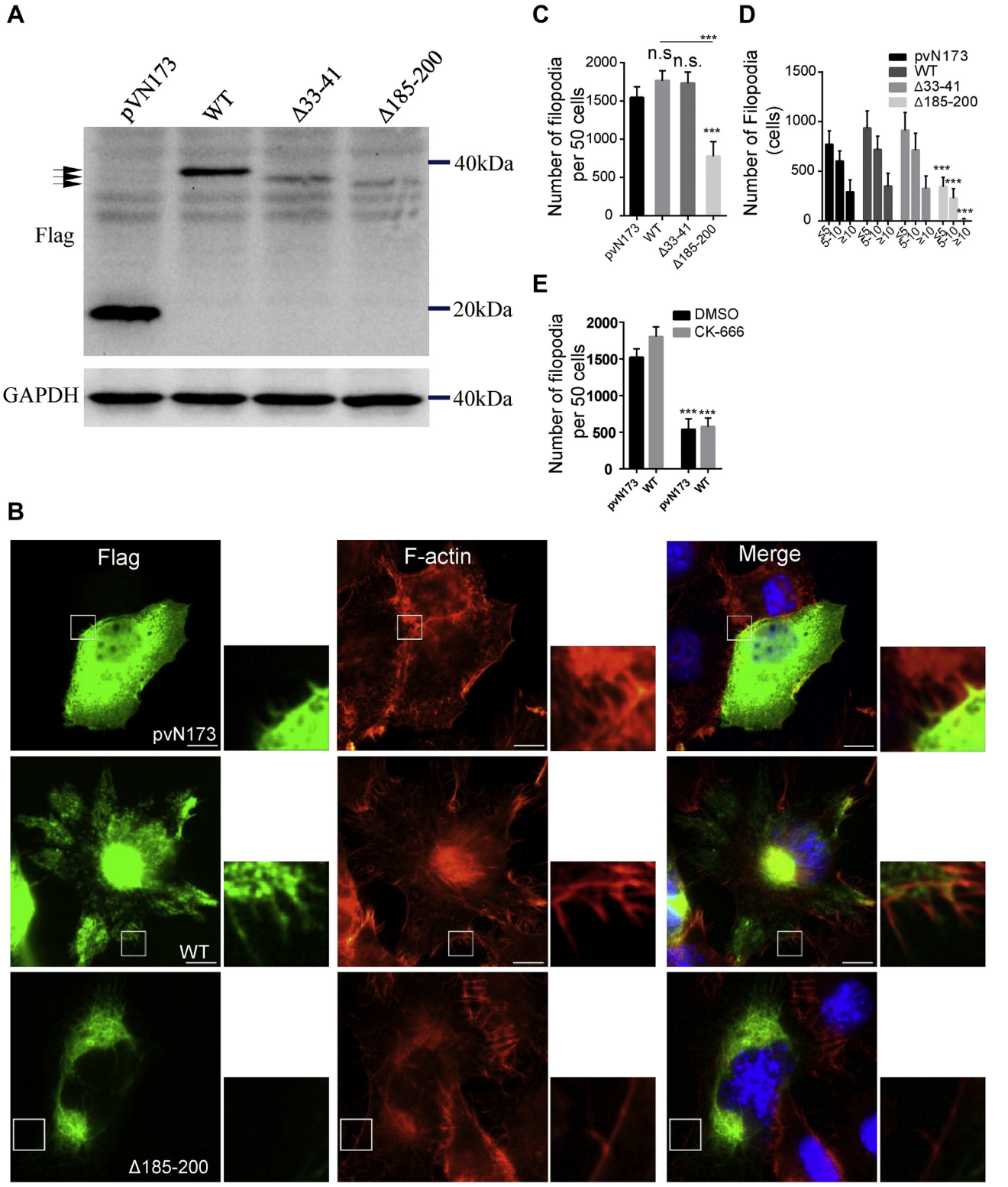

Figure 4 PRR11 induces the filopodia formation via proline rich region 2. (**A**) Western blot analysis for the indicated proteins. Cells were overexpressed with transient transfected pVN173, WT PRR11, Δ33-41 or Δ185-200, and then cells were fixed after 24 h. Cells were treated as (**D**) and then were lysed, and analyzed for expression of the indicated proteins by Western blotting. (**B**) The subcellular localization of WT PRR11 and Δ185-200. Cells were overexpressed with transient transfected pVN173, WT PRR11 or Δ185-200, and then cells were fixed after 24 h and stained for Flag and phalloidin. Representative images are shown. Bar, 10 μm. (**C, D**) Quantified of the number and length of filopodia in pVN173-, WT PRR11-, Δ33-41- or Δ185-200-expressing cells. The number and length of filopodia in pVN173-, WT PRR11-, Δ33-41-, or Δ185-200-transfected cells were evaluated by automated scanning using confocal microscopy. The length of filopodia was measured from the surface to the tip of the filopodia. Results are shown as the

migration and spreading.[8] Thus we presumed that PRR11 could regulate cell migration via the Arp2/3 complex in lung cancer cells. To examine this hypothesis, cells were transiently transfected with the control siRNA (siNC) or with siRNA against PRR11 (siPRR11). Forty-eight hours after transfection, whole cell lysates were prepared and subjected to immunoblotting analysis. As shown in Figure 1A, the amounts of PRR11 was significantly reduced at protein level under our experimental conditions. Silencing of PRR11 expression significantly increased cellular size in A549 and H1299 cells (Fig. 1B, C). In addition, 48 h after the siNC- and siPRR11-transfected, cells were placed into the 6 cm dish. Compared with the siNC-transfected cells, the A549 and H1299 cells increased attachment to dish in the siPRR11-transfected groups (Fig. 1D). Furthermore, the migration trajectories of A549 cells were recorded, and the velocity of cell migration and the distance from the origin were then analyzed with the ImageJ software. As expect, cell motility was remarkably decreased in the siPRR11-transfected cells compared to the siNC-transfected cells (Fig. 1E, F). And the distance and average speed were decreased in the siPRR11-transfected cells relative to the siNC-transfected cells (Fig. 1G). Our results demonstrated that silencing of PRR11 expression alter cell adhesion and cell motility in NSCLC cells.

PRR11 facilitates filopodia formation depending on its proline-rich region 2

Branched actin generated by the ARP2/3 complex localizes to the leading edge of migrating cells, which provides the protrusive force that is required to generate and extend distinct thin protrusions (the surface tentacles) known as the filopodia and the broad sheet-like protrusions known as the lamellipodia.[5] Then, whether PRR11 regulates the filopodia and/or lamellipodia formation via Arp2/3 complex. First, we examined localization of endogenous PRR11 and Arp2 by confocal microscopy. As shown in Figure 2A and B, endogenous PRR11 was significant enriched at the filopodia and co-localized with Arp2 (the white arrow), but not the lamellipodia, although ARP2 was also identified at the lamellipodia (the red arrow) in cultured A549 cells. Next, to determine whether PRR11 regulates the subcellular distribution of ARP2/3 complex, we examined localization of Arp2 in the siPRR11-transfected cells. Anti-Arp2 immunofluorescence staining showed that fluorescence signal of the surface tentacles is significantly reduced in the siPRR11-transfected cells, whereas, the localization of Arp2 at the lamellipodia is not altered (Fig. 2A). It suggested that PRR11-depeltion disrupts the localization of Arp2 at the surface tentacles and could repress filopodia formation. In line with our previous studies,[16] immunoblots confirmed that silencing of PRR11 also reduced the level of endogenous Arp2 (data not shown).

In order to further investigate whether PRR11 is required for filopodia formation via ARP2/3 complex, we detected the actin filaments assembly of filopodia in response to PRR11 silencing. The silencing efficiency of siRNA was detected by immunoblotting analysis (Fig. 3A). Using immunofluorescence staining, we observed that the surface tentacles in siNC-transfected cells were intensely stained with rhodamine phalloidin (red), indicative F-actin filopodia. However, the surface tentacles were remarkably decreased in the siPRR11-transfected cells (Fig. 3B). In line with our previous studies,[16] immunofluorescence staining also showed a decreased fluorescence signal of F-actin and an increased number of stress fibers following PRR11 siRNA treatment (Fig. 3B, C). Next, we quantified the number and length of filopodia in the siNC- and siPRR11-transfected cells by automated scanning. We counted all filopodia from, on average, 50 cells per treatment per experiment, and the length of each tentacle was measured from the cell surface to the tip of the tentacle. The number and length of filopodia from three independent experiments are summarized in Figure 3D and E. We found that the number of filopodia is remarkably reduced in PRR11-depletion cells compared to siNC cells (Fig. 3D). And the length of ~65% filopodia was identified longer than 5 μm in the siNC-transfected cells, whereas, the number of long filopodia (≥5 μm) was greatly reduced in siPRR11-transfected cells (Fig. 3E). In addition, we also characterized the role of ARPC1A, which has been known a subunit of ARP2/3 complex to stimulate actin polymerization. The amounts of ARPC1A was significantly reduced at protein levels by against ARPC1A siRNA (Fig. 3A). Furthermore, the number and length of surface tentacles were also reduced in the ARPC1A-depletion cells compared with siNC-transfected cells (Fig. 3B—E), confirming that the depletion of key factor involved in filopodia formation has a similar effect as PRR11 depletion. Due to the effect of siPRR11 and siARPC1A may be unsustainable and unstable. To confirm these finding, we used A549 to establish PRR11 and ARPC1A stable knockdown cell lines. Western blot analysis demonstrated that the PRR11 or ARPC1A expression was significantly silenced at protein levels in the stable PRR11 or ARPC1A knockdown cells (Fig. S1A). Consistent with the phenotypes observed in transient knockdown experiments (Fig. 3B—D), stable knockdown of PRR11 or ARPC1A also caused a significant decreased of the number and length of surface tentacles (Fig. S2B, C). Taken together, these results confirm that PRR11 implicates in Arp2-mediating filopodia formation in NSCLC cells.

Our previous studies have demonstrated that PRR11 regulates F-actin polymerization and arrangement via different region. The role of PRR11 on nuclear integrity depends on its N and C termini-mediated cytoskeleton assembly, and the proline-rich region 2 deletion mutant stimulates actin filaments polymerization, but weakly

mean ± S.E, ($n = 3$). Greater than 50 cells were counted per condition in every repeat. *n.s, $P > 0.05$; ***, $P < 0.001$.* (E) Quantified of the number of filopodia in pVN173- and WT PRR1-expressing cells combined with inhibitor treatment. Cells were transiently transfected pVN173- and WT PRR11. Four to 6 h after transfection, cells were treated with ARP2/3 complex inhibitor (CK666, final concentration of 84 μM) for 48 h. The number of filopodia in pVN173- and WT PRR11-transfected cells were evaluated by automated scanning using confocal microscopy. Results are shown as the mean ± S.E. ($n = 3$). Greater than 50 cells were counted per condition in every repeat. *n.s, $P > 0.05$; ***, $P < 0.001$.*

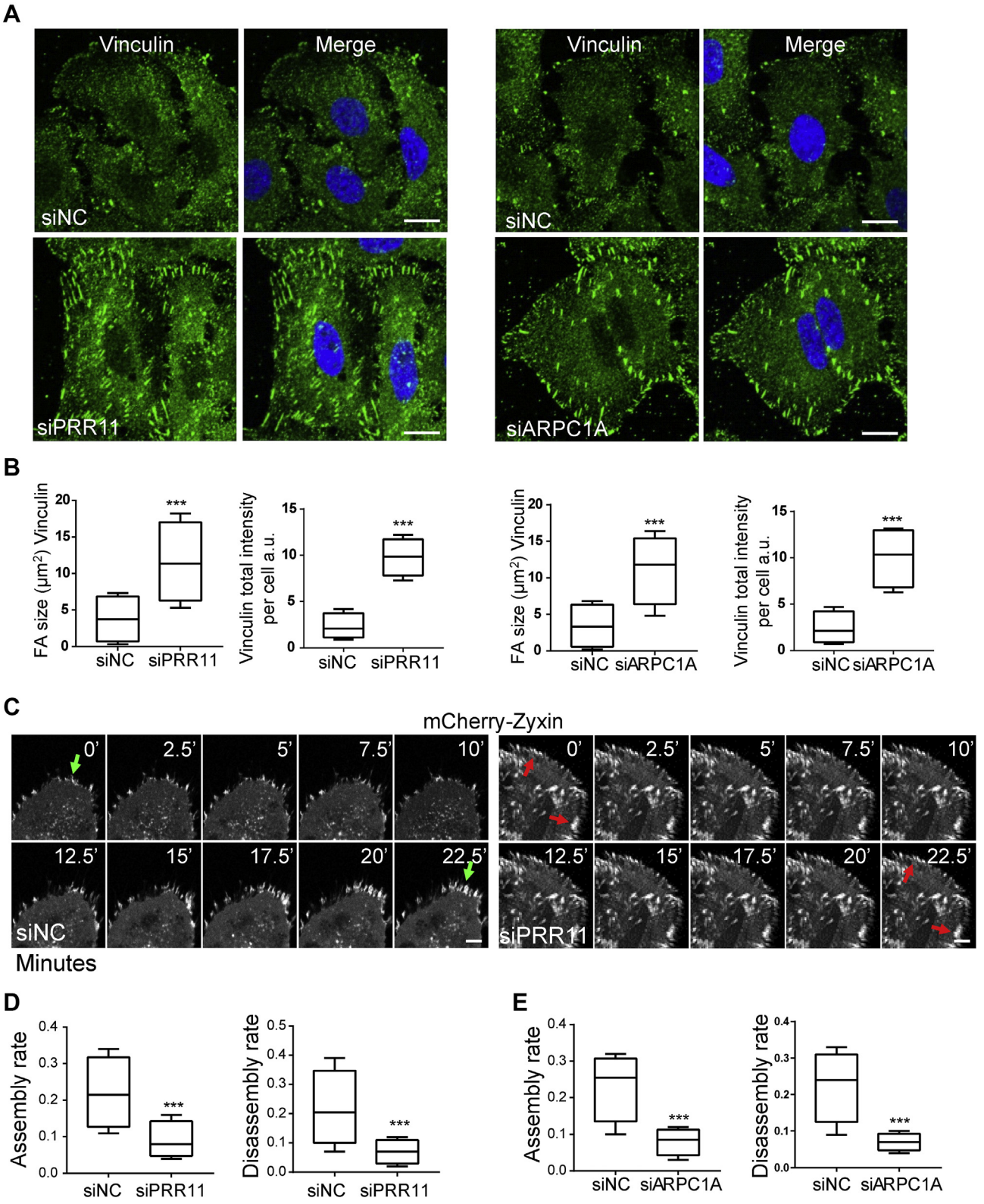

Figure 5 PRR11 regulates focal adhesion turnover dynamic in NSCLC cells. (**A**) Immunolabeling for focal adhesions marker vinculin in the siNC-, siPRR11-and ARPC1A-transfected cells. Cells were transiently transfected with siNC or siRNA directed against PRR11 and ARPC1A. Forty-eight hours after transfection, cells were fixed and stained with vinculin antiboby. Representative images are shown. Cell nuclei were stained with DAPI (blue). Bars, 10 μm. (**B**) Quantitated of the size and total fluorescence intensity of vinculin. A549 cells were transiently transfected as in (**A**). Box-and-whisker plot indicating the size and total fluorescence staining intensity of focal adhesions in the siNC-, siPRR11-and siARPC1A-transfected cells, respectively. $n = 3$. Greater than 20 cells were counted per condition in every repeat. *a.u.*, *arbitrary units*. ***, $P < 0.001$. (**C**—**E**) Focal adhesions turnover in the siRNA transfected

effects on actin arrangement.[16] Next, we examined whether ectopic expression of WT PRR11 and truncated mutations affect filopodia formation in A549 cells. The overexpression of pvN173 (Flag-tagged N-terminal 173 residues of enhanced GFP), WT-PRR11 and truncations absence of proline-rich region 1 (Δ33—41), and absence of proline-rich region 2 (Δ185-200) was confirm by Western blot (Fig. 4A). As shown in Fig. 4B, the fluorescence signal of WT PRR11 could be detected at the whole filopodia (containing the tip and base of filopodia) in the medium and low level expression of ectopic WT PRR11 cells. Moreover, we found that Δ33—41 showed similar phenotype to WT PRR11 (data not shown). However, the fluorescence signal were not identified at the filopodia in Δ185-200-expressing cells and the fluorescence signal was just found at the basal filopodia in pvN173-control cells (Fig. 4B). In line with our previous studies, Δ185-200 overexpression cells just induced thick actin filaments in the perinuclear (Fig. 4B).[16] Consequently, we quantified the number and length of filopodia in the pvN173-, WT PRR11-, Δ33-41- and Δ185-200-expressing cells. Compared to pvN173-expressing cells, the number of filopodia was remarkably increased in WT PRR11 and Δ33-41 ectopic expression cells, whereas, Δ185-200-expressing cells showed filopodia reduction: in some cells, the cell surface appeared to be completely devoid of filopodia, while in other cells filopodia were present, but the number and length were decreased (Fig. 4C). In addition, in WT PRR11 overexpression cells, the number of longer filopodia was greatly raised compared with pvN173 cells (Fig. 3D). To further confirm that PRR11 promotes the filopodia formation depending on Arp2/3 complex-induced actin filaments assembly, we next employed the CK-666 (the Arp2/3 complex inhibitor) to repress actin filaments polymerization. In keeping with the siRNA-mediated knockdown experiments, CK-666 also gave rise to an inhibition of WT PRR11 overexpression induced filopodia formation, whereas DMSO did not (Fig. 3E). These data suggested that WT PRR11 overexpression facilitates filopodia formation, and the proline-rich 2 domain is essential for PRR11 subcellular colocalization and induces the generation of filopodia via ARP2/3 complex in NSCLC cells.

Depletion of PRR11 inhibits focal adhesion turnover in NSCLC cells

Filopodia are dynamic plasma membrane protrusion filled with actin filaments and involved in the formation of focal adhesion to the ECM.[4,5] Dysregulation of F-actin assembly disrupts focal adhesions turnover and results in aberrant cell motility.[6,9,17] To further determine the role of PRR11 in focal adhesions turnover, we examined whether depletion of PRR11 affected cell focal adhesions dynamic. In the siPRR11-transfected cells, we observed the number and the size of vinculin, the marker of focal adhesion, was significantly increased relative to siNC-transfected cells (Fig. 5A, B). Furthermore, anti-vinculin immunofluorescence staining also showed ARPC1A-silencing cells had a greater number of larger, more brightly stained focal adhesions relative to siNC-transfected cells (Fig. 5A, B). We further used confocal videomicroscopy to trace and examine the trajectory of individual focal adhesions.[18] To visualize Focal adhesions, we generated a stable overexpresssion mCherry-Zyxin A549 cell line, a fluorescently labeled focal adhesions marker protein.[18,19] Representative figures of the perturbations in focal adhesions dynamics arising from siNC- and siPRR11-transfected cells are shown in complete form in montages in Figure 5C. During the interval of observation, focal adhesions in siPRR11-transfected cells were often static, while many focal adhesions in siNC-transfected cells underwent continual bouts of formation, maturation, and disassembly. Quantification of the kinetics of individual focal adhesions revealed a dramatic decrease in both the assembly and disassembly rates of focal adhesions in PRR11-depletion cells (Fig. 5D). In keeping with the siRNA-mediated knockdown PRR11, silencing of ARPC1A also gave rise to an inhibition of focal adhesions turnover (Fig. 5E). Taken together, these data suggested that PRR11 regulates focal adhesions turnover by controlling filopodia formation to effect on cell adhesion and cell motility in NSCLC cells.

PRR11-depletion reduces integrin β1 internalization and represses phosphorylation of FAK^{Y397} in NSCLC cells

Focal adhesions physically connect the ECM to the actin cytoskeleton through transmembrane receptor integrins and provides essential signals for cell migration.[7] Integrins are heterodimers consisting of α and β subunits and can be activated by the binding of specific activators trigging the formation of focal adhesion.[20] The internalization and intracellular trafficking of integrin which is one of the first targets regulated by actin filaments is implicated in cell motility.[7] However, whether the filopodia actin network regulates integrin internalization remains poorly understood in NSCLC cells. On the cellular surface, integrins are in an allosteric equilibrium between an inactive and an active conformation that respectively interact at a low and high affinity with ligands.[7] Recent data suggested that dysregulation of actin cytoskeleton increases the cell

cells. mCherry-Zyxin-expressing A549 cells were transiently transfected as in (**A**). Forty-eight hours after transfection, cells were placed into the confocal dish to photograph by confocal microscopy. (**C**) Representative time-lapse images (montages) of mCherry-Zyxin-expressing (the fluorescently labeled focal adhesions marker protein) in the siNC- and siPRR11-transfected cells. Scale bar, 10 μm. (**D**) Box-and-whisker plots revealing slow assembly and disassembly rates of focal adhesions in siPRR11 cells relative to their siNC counterparts. Note formation and dissolution of focal adhesions in the siNC transfected cells and very static focal adhesions in siPRR11-transfected cells. $n = 3$. Greater than 50 cells were counted per condition in every repeat. (**E**) Box-and-whisker plots revealing slow assembly and disassembly rates of focal adhesions in siARPC1A cells relative to their siNC counterparts in keeping with the siRNA-mediated knockdown PRR11. $n = 3$. Greater than 50 cells were counted per condition in every repeat. ***, $P < 0.001$.

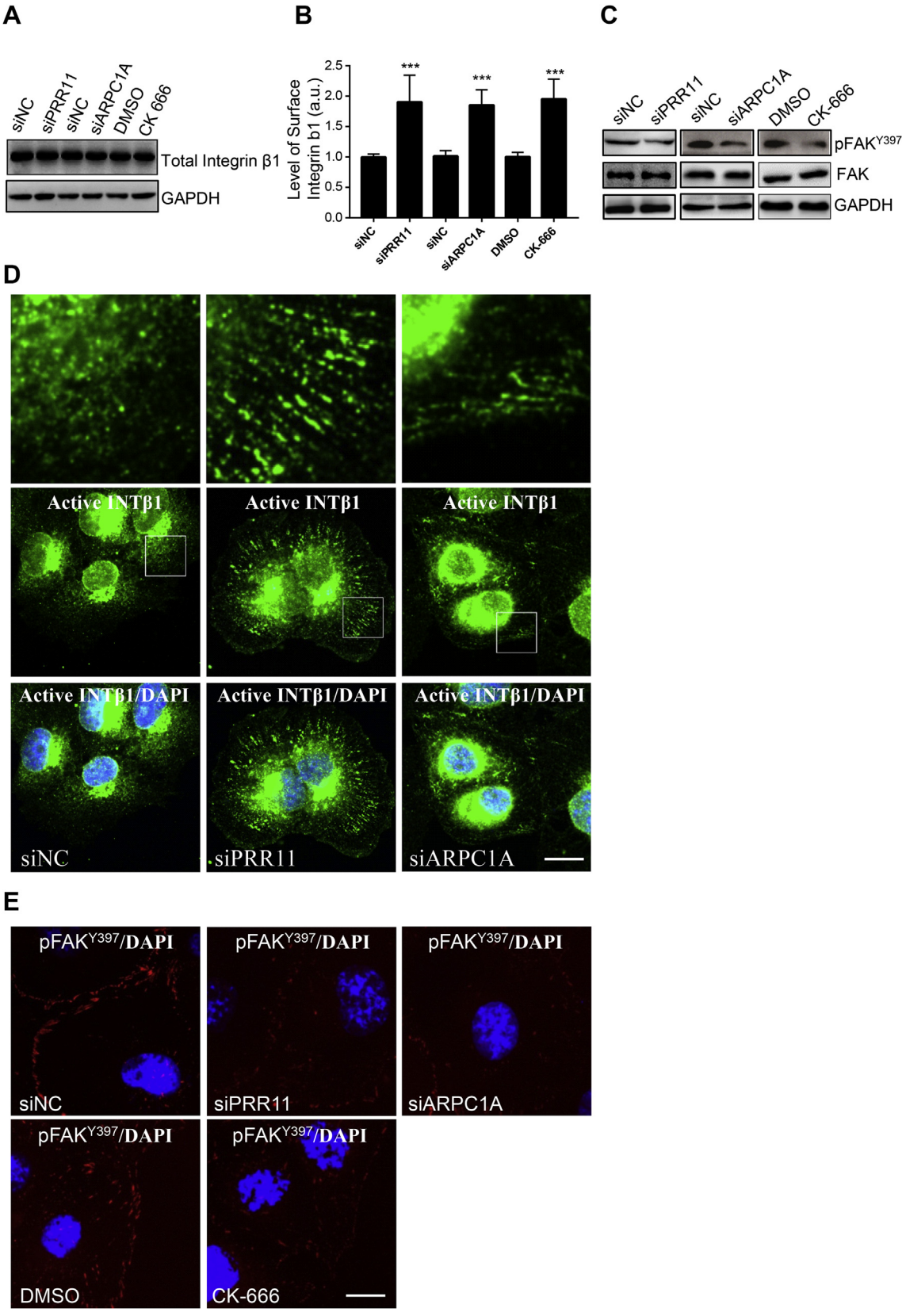

Figure 6 PRR11 regulates internalization of integrin β1 and phosphorylation of FAK^{Y397} depending on ARP2/3 complex in NSCLC cells. (**A**) Western blot analysis for the total level of integrin β1. A549 cells were treated with siRNA transiently transfected (siNC, siPRR11 or siARPC1A) or ARP2/3 complex inhibitor treatment with a final concentration of 84 μM (CK666) for 48 h, respectively. And then cells were lysed and analyzed for the indicated proteins. (**B**) Quantitated of the surface expression of integrin β1 by flow

surface active integrin β1 level and decreases integrin internalization, which has critical roles in inhibiting cell migration.[19,21] To determine the role of PRR11 in this process, we first detected the total integrin β1. Immunoblotting of cell lysates demonstrated that overall level of integrin β1 is not changed in PRR11- and ARPC1A-depletion as well as CK-666 treatment cells compared to siNC-transfected or DMSO treatment cells (Fig. 6A). Next, we quantitated the surface expression of endogenous integrin β1 by flow cytometry after siRNA-transfected or inhibitor treatment in A549 cells. Results indicated that silencing of PRR11 and ARPC1A or inhibition of actin filaments assembly by CK-666 treatment induces an increase in surface level of active integrin β1 relative to siNC-transfected or DMSO treatment cells (Fig. 6B). As we know that FAK signaling is strongly dependent on integrin internalization and implicates in focal adhesions turnover, which one of the first downstream components to become activated by integrin.[7,22] Consequently, we detected the total expression of FAK and the level of FAK^{Y397} 48 h after siRNA-transfected and CK-666 treatment. Immunoblotting of cell lysates demonstrated that FAK^{Y397} is significantly reduced, however, overall expression of FAK was not changed by silencing of PRR11 and ARPC1A or CK-666 treatment (Fig. 6C). In addition, staining of active integrin β1 showed an increase in the number of long FAs by immunofluorescence staining (Fig. 6D). And then immunofluorescence staining also showed a decrease in the level of FAK^{Y397} in depletion of PRR11 and ARPC1A as well as CK-666 treatment relative to control cells (Fig. 6E). In line with this, stable knockdown of PRR11 or ARPC1A also caused remarkably increased surface level of active integrin β1 by flow cytometry, and the inhibited level of FAK^{Y397} by immunofluorescence staining (Fig. S2A, B). Our previous work has demonstrated that PRR11 was overexpressed in lung cancer tissues as compared with normal lung tissues.[10] Reports have also revealed the overexpression of FAK and phosphorylated FAK^{Y397} in NSCLC cancers.[23] Finally, to obtain further insight into the expression correlation of PRR11 and FAK^{Y397} in NSCLC tissue by immunohistochemistry analysis of NSCLC tissue microarray. A weaker positive correlation between the PRR11 and FAK^{Y397} was evaluated in NSCLC tissues, though there is not statistically significant (Fig. 7A, $P = 0.0525$, Table S3). Taken together, our results provide evidence that PRR11 could effect on integrin-FAK pathway to promote focal adhesions dynamics via ARP2/3 complex.

Discussion

PRR11 is overexpressed in lung cancers and has important roles in tumorigenesis.[10] Silencing of PRR11 inhibits cell proliferation and migration in various cancer cells.[10,13,15] However, the molecular mechanisms underlying these events remain elusive. We have previously demonstrated that PRR11 interacts with and recruits the Arp2/3 complex to control nuclear lamina integrity and chromatin remodeling by driving F-actin polymerization and rearrangement.[16] In this study, we have demonstrated that PRR11 effects on filopodia formation via recruiting Arp2/3 complex, thereby regulating membrane protrusions and focal adhesions turnover to control cell motility in NSCLC cells. Our findings have uncovered the molecular mechanisms that PRR11 regulates Arp2/3 complex-mediated filopodia formation, focal adhesion dynamic and cell motility via the actin cytoskeleton (Fig. 7B).

The actin cytoskeleton is outstandingly dynamic, and different actin filaments polymerization can generate a variety of architectures, which is tightly controlled by actin-nucleating proteins such as the Arp2/3 complex, formins and Ena/VASP.[3,4,8] The plasma membrane protrusions at the leading edge of a migrating or an elongating cell are called lamellipodia and filopodia resulting from actin filaments assembly.[4] Filopodia are highly dynamic and have various functions, such as adhesion to the extracellular matrix, cell mobility, embryonic development and tumorigenesis, thereby implicating in process of physiology and pathology.[5] A large number of proteins that control the actin filaments dynamic have been shown to localize to filopodia and to promote filopodia formation such as Rac1, formins, Ena/VASP, Myosin-X and Arp2/3 complex.[5] However, these proteins seem to contribute to the generation of filopodia in specific cell types. Filopodia could be derived from the lamellipodia actin network which depends on Arp2/3 complex, or be nucleated at filopodia tips by formins.[5] Previously our studies have demonstrated that PRR11 associates with and recruits the ARP2/3 complex to regulate cytoskeleton-nucleoskeleton assembly in NSCLC cells.[16] In this study, we further reveal that PRR11 enriches at the filopodia and promotes filopodia formation by recruiting ARP2/3 complex. We demonstrated that PRR11 depletion or overexpression inhibits or increases Arp2 localizing to filopodia, and also represses or induces filopodial formation, respectively. Interestingly, Mehedi M et al., also found that the Arp2/3 complex has an important role in human respiratory syncytial virus-induced filopodia formation.[24] Furthermore, we also found that the proline-rich 2 domain is essential for PRR11 inducing the filopodia formation, although, it is dispensable for actin filaments assembly. Taken together, we hypothesized that PRR11 involves in generation of filopodia resulting from recruiting Arp2/3 complex to promote actin filaments assembly in NSCLC cells.

In migrating cells, filopodia and lamellipodia is initiated by actin filaments assembly at the leading edge,

cytometry. A549 cells were treated as in (**A**). Surface level of activated integrin β1 was immunofluorescence staining via mouse monoclonal antibodies against activated integrin β1 and was determined by flow cytometry. Results are shown as the mean ± S.E. ($n = 3$). *a.u., arbitrary units*. ***, $P < 0.001$. (**C**) Western blot analysis for the indicated proteins. A549 cells were treated as in (**A**). And then cells were lysed and analyzed for the indicated proteins. (**D**) Immunofluorescence staining for active integrin β1 A549. Cells were treated as in (**A**), and then stained for active integrin β1 (green). Representative images are shown. Cell nuclei were stained with DAPI (blue). Bar, 10 μm. (**E**) Detected the level of $pFAK^{Y397}$ by immunofluorescence staining. A549 cells were treated as (**A**). Then cells were fixed and stained with $pFAK^{Y397}$ antibody. Representative images are shown. Cell nuclei were stained with DAPI (blue). Bar, 10 μm.

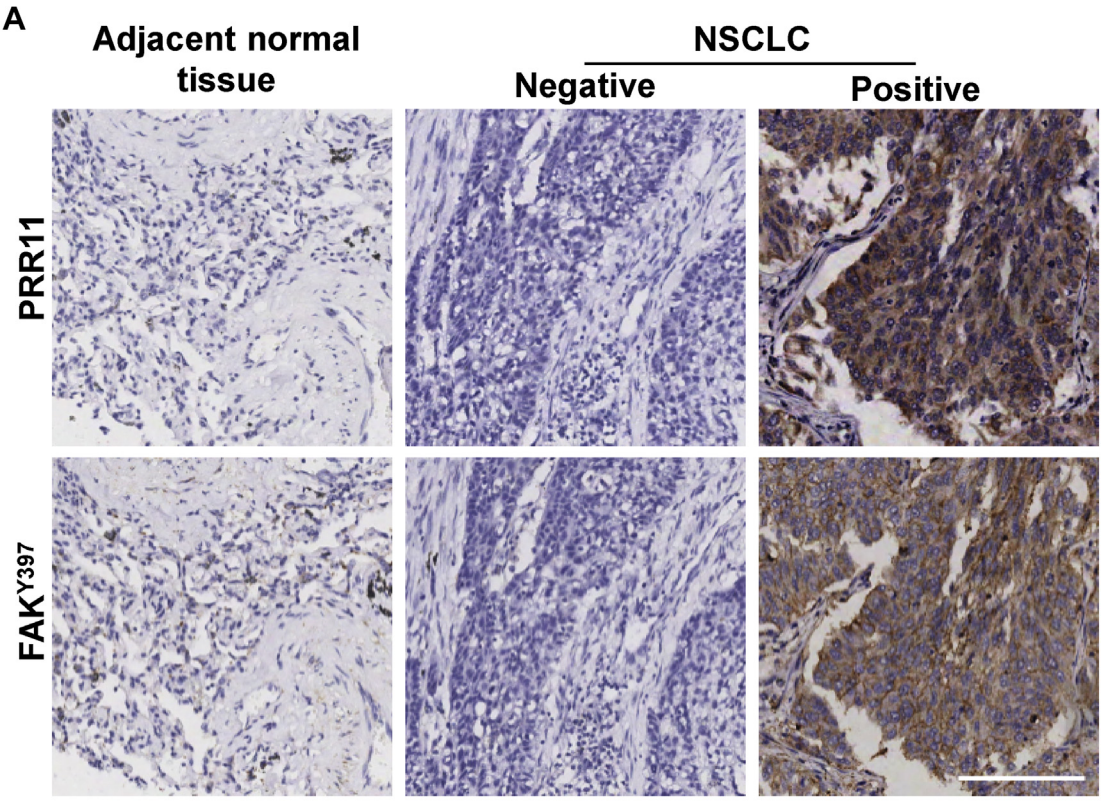

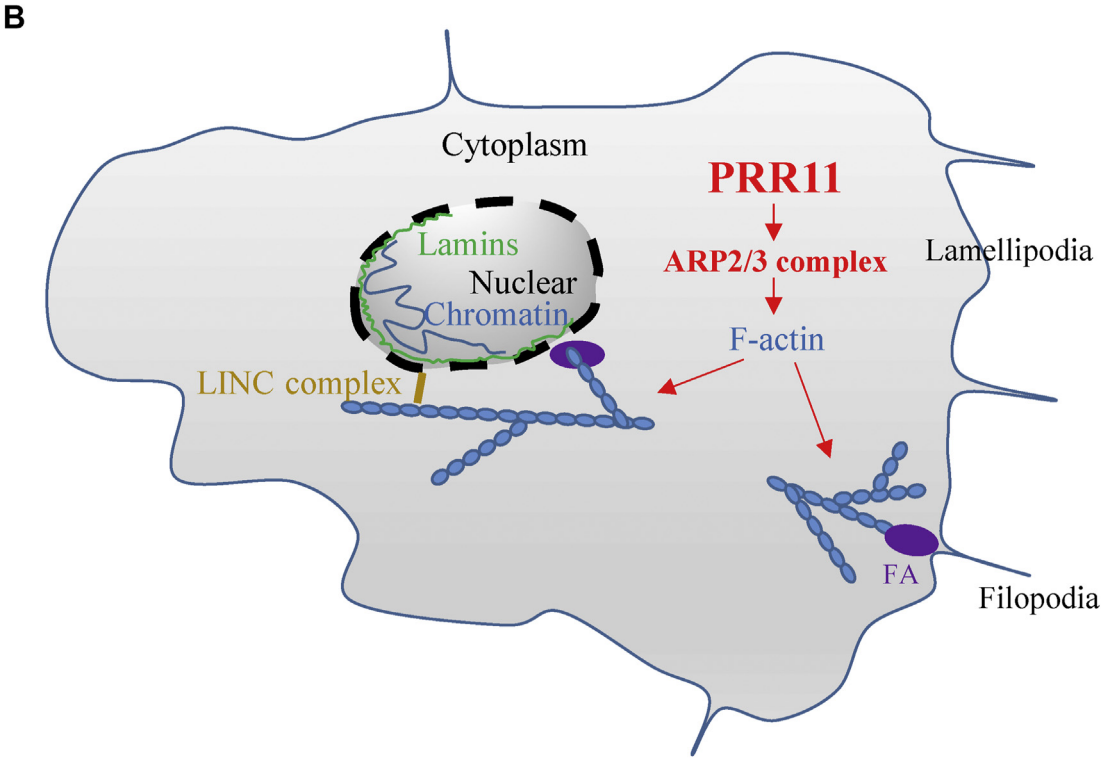

Figure 7 The expression of PRR11 and FAK^{Y397} in NSCLC cells. (**A**) Expression of PRR11 and FAK^{Y397} was examined by immunohistochemistry in NSCLC. Bar, 100 μm. (**B**) Proposed working model. PRR11 associates with and recruits Arp2/3 complex to facilitate F-actin assembly and rearrangement, thereby to control fiopodia formation, but not lamellipodia. PRR11-ARP2/3 complex also implicates in regulation nuclear lamina integrity, which might be mediated by the LINC complex coupling both nuclear lamina and actin cytoskeleton.

following adhesions-substratum are formed to stabilize connection of filopodia and/or lamellipodia to the ECM by focal adhesions.[3,4,6] Focal adhesions are integrin-based, complex structures situated at the cell base that mediate cell-substratum adhesion by connecting the ECM to the actin cytoskeleton.[6] Integrins can be bidirectionally activated by the binding of specific activators to integrin cytoplasmic tails or by binding of ECM components.[6] Cell migration depends on membrane spreading induced by actin filaments polymerization and a series of assembly and disassembly events of integrin-mediated focal adhesions.[6,7] A number of reports have been demonstrated that actin filaments couples with focal adhesions turnover dynamic by regulating integrin internalization, degradation or phosphorylation of accessary proteins such as FAK, which corresponds to the strong—or weak-adhesion state to regulate cell movement.[7] Our results indicated that silencing of PRR11 expression induces larger cellular size and inhibits cell motility and focal adhesions turnover dynamic. PRR11 depletion also leads to an increase in surface level of active integrin β1 relative to control cells, suggesting that PRR11 potentially regulates integrin internalization via Arp2/3 complex in NSCLC cells. In line with this, we demonstrated that silencing of PRR11 expression also repress the level of pFAK-Y397, but not total level of FAK in NSCLC cells. FAK exists in an autoinhibited conformation in the cytoplasm, however, actin filaments flow, integrins internalization and/or other proteins stimulates relieves the atuophosphorylated by triggering atuophosphorylation of Y397 in trans.[7,25] Alanko, j. et al., demonstrated that inhibition of integrin internalization reduced integrin-mediated $pFAK^{Y397}$.[22] Our studies suggested that PRR11 potentially effects on cell motility via Arp2/3 complex to regulate focal adhesions turnover dynamic by controlling actin filaments assembly of filopodia.

Taken together, our results demonstrated that PRR11-ARP2/3 complex axis effects on actin filaments assembly of filopodium protrusion to regulate focal adhesions turnover dynamic and cell mobility by controlling integrin internalization and phosphorylation of FAK in NSCLC cells.

Conflict of interests

The authors declare that they have no conflict of interest.

Funding

This work was supported in part by a grant-in-aid from the National Natural Science Foundation of China (No. 81773040 to JG and 81501979 to CZ, http://www.nsfc.gov.cn/), and the Chongqing Science and Technology Commission (No. cstc2018jcyj-yszxX0011 to JG and cstc2017jcyjAX0464 to CZ) and the Scientific and Technological Research Projects of Chongqing Education Commission (No. KJQN201800423 to CZ). The funders had no role in study design, data collection and analysis, decision to publish, or preparation of the manuscript.

Appendix A. Supplementary data

Supplementary data to this article can be found online at https://doi.org/10.1016/j.gendis.2021.02.012.

References

1. Siegel RL, Miller KD, Jemal A. Cancer statistics, 2018. *CA Cancer J Clin*. 2018;68(1):7—30.
2. Herbst RS, Morgensztern D, Boshoff C. The biology and management of non-small cell lung cancer. *Nature*. 2018;553(7689):446—454.
3. Caswell PT, Zech T. Actin-based cell protrusion in a 3D matrix. *Trends Cell Biol*. 2018;28(10):823—834.
4. Ridley AJ. Life at the leading edge. *Cell*. 2011;145(7):1012—1022.
5. Mattila PK, Lappalainen P. Filopodia: molecular architecture and cellular functions. *Nat Rev Mol Cell Biol*. 2008;9(6):446—454.
6. Wehrle-Haller B. Structure and function of focal adhesions. *Curr Opin Cell Biol*. 2012;24(1):116—124.
7. Alanko J, Ivaska J. Endosomes: emerging platforms for integrin-mediated FAK signalling. *Trends Cell Biol*. 2016;26(6):391—398.
8. Rotty JD, Wu C, Bear JE. New insights into the regulation and cellular functions of the ARP2/3 complex. *Nat Rev Mol Cell Biol*. 2013;14(1):7—12.
9. Bugyi B, Carlier MF. Control of actin filament treadmilling in cell motility. *Annu Rev Biophys*. 2010;39:449—470.
10. Ji Y, Xie M, Lan H, et al. PRR11 is a novel gene implicated in cell cycle progression and lung cancer. *Int J Biochem Cell Biol*. 2013;45(3):645—656.
11. Zhang C, Zhang Y, Li Y, et al. PRR11 regulates late-S to G2/M phase progression and induces premature chromatin condensation (PCC). *Biochem Biophys Res Commun*. 2015;458(3):501—508.
12. Zhang L, Lei Y, Zhang Y, et al. Silencing of PRR11 suppresses cell proliferation and induces autophagy in NSCLC cells. *Genes Dis*. 2018;5(2):158—166.
13. Chen Y, Cha Z, Fang W, et al. The prognostic potential and oncogenic effects of PRR11 expression in hilar cholangiocarcinoma. *Oncotarget*. 2015;6(24):20419—20433.
14. Wang Y, Zhang C, Mai L, Niu Y, Wang Y, Bu Y. PRR11 and SKA2 gene pair is overexpressed and regulated by p53 in breast cancer. *BMB Rep*. 2019;52(2):157—162.
15. Song Z, Liu W, Xiao Y, et al. PRR11 is a prognostic marker and potential oncogene in patients with gastric cancer. *PloS One*. 2015;10(8):e0128943.
16. Zhang L, Zhang Y, Lei Y, et al. Proline-rich 11 (PRR11) drives F-actin assembly by recruiting the actin-related protein 2/3 complex in human non-small cell lung carcinoma. *J Biol Chem*. 2020;295(16):5335—5349.
17. Salmon WC, Adams MC, Waterman-Storer CM. Dual-wavelength fluorescent speckle microscopy reveals coupling of microtubule and actin movements in migrating cells. *J Cell Biol*. 2002;158(1):31—37.
18. Wu X, Kodama A, Fuchs E. ACF7 regulates cytoskeletal-focal adhesion dynamics and migration and has ATPase activity. *Cell*. 2008;135(1):137—148.

19. Yue J, Xie M, Gou X, Lee P, Schneider MD, Wu X. Microtubules regulate focal adhesion dynamics through MAP4K4. *Dev Cell*. 2014;31(5):572—585.
20. Harburger DS, Calderwood DA. Integrin signalling at a glance. *J Cell Sci*. 2009;122(Pt 2):159—163.
21. D'Souza-Schorey C, Chavrier P. ARF proteins: roles in membrane traffic and beyond. *Nat Rev Mol Cell Biol*. 2006;7(5):347—358.
22. Alanko J, Mai A, Jacquemet G, et al. Integrin endosomal signalling suppresses anoikis. *Nat Cell Biol*. 2015;17(11):1412—1421.
23. Wang B, Qi X, Li D, Feng M, Meng X, Fu S. Expression of pY397 FAK promotes the development of non-small cell lung cancer. *Oncol Lett*. 2016;11(2):979—983.
24. Mehedi M, McCarty T, Martin SE, et al. Actin-related protein 2 (ARP2) and virus-induced filopodia facilitate human respiratory syncytial virus spread. *PLoS Pathog*. 2016;12(12):e1006062.
25. Cai X, Lietha D, Ceccarelli DF, et al. Spatial and temporal regulation of focal adhesion kinase activity in living cells. *Mol Cell Biol*. 2008;28(1):201—214.